Nuclear Medicine and Biology 43 (2016) 732–741

Contents lists available at ScienceDirect

Nuclear Medicine and Biology

journal homepage: www.elsevier.com/locate/nucmedbio

Novel ^{99m}Tc(III)-azide complexes [^{99m}Tc(N$_3$)(CDO)(CDOH)$_2$B-R] (CDOH$_2$ = cyclohexanedione dioxime) as potential radiotracers for heart imaging

Min Liu [a,b], Yumin Zheng [c], Ugur Avcibasi [b,d], Shuang Liu [b,*]

[a] Department of Radiation Medicine and Protection, Medical College, Soochow University, China
[b] School of Health Sciences, Purdue University, IN, 47907, USA
[c] Department of Nuclear Medicine, China–Japan Friendship Hospital, Beijing, 100037, China
[d] Department of Chemistry, Faculty of Arts and Science, Celal Bayar University, 45040, Yunusemre/Manisa, Turkey

ARTICLE INFO

Article history:
Received 27 April 2016
Accepted 2 May 2016
Available online xxxx

Keywords:
^{99m}Tc-Teboroxime derivatives
^{99m}Tc radiotracers
heart imaging

ABSTRACT

Introduction: In this study, novel ^{99m}Tc(III)-azide complexes [^{99m}Tc(N$_3$)(CDO)(CDOH)$_2$B-R] (^{99m}Tc-ISboroxime-N$_3$: R = IS; ^{99m}Tc-MPboroxime-N$_3$: R = MP; ^{99m}Tc-PAboroxime-N$_3$: R = PA; ^{99m}Tc-PYboroxime-N$_3$: R = PY; and ^{99m}Tc-Uboroxime-N$_3$: R = 5U) were evaluated as heart imaging agents.

Methods: Complexes [^{99m}Tc(N$_3$)(CDO)(CDOH)$_2$B-R] (R = IS, MP, PA, PY and 5U) were prepared by ligand exchange between NaN$_3$ and [^{99m}TcCl(CDO)(CDOH)$_2$B-R]. Biodistribution and imaging studies were carried out in Sprague–Dawley rats. Image quantification was performed to compare their initial heart uptake and myocardial retention.

Results: ^{99m}Tc-ISboroxime-N$_3$, ^{99m}Tc-PYboroxime-N$_3$ and ^{99m}Tc-Uboroxime-N$_3$ were prepared with high RCP (93–98%) while the RCP of ^{99m}Tc-MPboroxime-N$_3$ and ^{99m}Tc-PAboroxime-N$_3$ was 80–85%. The myocardial retention curves of ^{99m}Tc-ISboroxime-N$_3$, ^{99m}Tc-PYboroxime-N$_3$ and ^{99m}Tc-Uboroxime-N$_3$ were best fitted to the bi-exponential decay function. The half-time of the fast component was 1.6 ± 0.4 min for ^{99m}Tc-ISboroxime-N$_3$, 0.7 ± 0.1 min for ^{99m}Tc-PYboroxime-N$_3$ and 0.9 ± 0.4 min for ^{99m}Tc-Uboroxime-N$_3$. The 2-min heart uptake from biodistribution studies followed the ranking order of ^{99m}Tc-ISboroxime-N$_3$ (3.60 ± 0.68%ID/g) > ^{99m}Tc-PYboroxime-N$_3$ (2.35 ± 0.37%ID/g) ≫ ^{99m}Tc-Uboroxime-N$_3$ (1.29 ± 0.06%ID/g). ^{99m}Tc-ISboroxime-N$_3$ had the highest 2-min heart uptake among ^{99m}Tc radiotracers revaluated in SD rats. High quality SPECT images were obtained with the right and left ventricular walls being clearly delineated. The best image acquisition window was 0–5 min for ^{99m}Tc-ISboroxime-N$_3$.

Conclusion: Both azide coligand and boronate caps had significant impact on the heart uptake and myocardial retention of complexes [^{99m}Tc(N$_3$)(CDO)(CDOH)$_2$B-R]. Among the radiotracers evaluated in SD rats, ^{99m}Tc-ISboroxime-N$_3$ has the highest initial heart uptake with the heart retention comparable to that of ^{99m}Tc-Teboroxime. ^{99m}Tc-ISboroxime-N$_3$ is a promising alternative to ^{99m}Tc-Teboroxime for SPECT MPI.

1. Introduction

Coronary artery disease (CAD) is a leading cause of premature death and permanent disability. Myocardial perfusion imaging (MPI) with radiotracers is an integral component in evaluation of the patients with known or suspected CAD [1–10]. If the patient has CAD, there will be an area with the reduced radiotracer uptake in the myocardium in response to reduced blood flow. If the reduced uptake is worse under stress conditions than that at rest, the perfusion defect is most likely due to ischemia. If the reduced uptake is the same under stress and at rest conditions, the perfusion defect is most likely caused by myocardial infarction. In order to evaluate areas with accuracy, the radiotracer must be taken up into myocardium in proportion to the regional blood flow rate [3–10]. Precise measurement of regional blood flow has significant clinical importance in identifying the ischemia, defining the extent and

Abbreviations: CAD, coronary artery disease; CT, computed tomography; CZT, cadmium-zinc-telluride; DTPA, diethylenetriaminepentaacetic acid; ITLC, instant thin layer chromatography; RCP, radiochemical purity; SPECT, single photon-emission computed tomography; ^{99m}Tc-ISboroxime, [^{99m}TcCl(CDO)(CDOH)$_2$B-IS] (CDOH$_2$ = cyclohexanedione dioxime, IS = isoxazol-4-yl); ^{99m}Tc-ISboroxime-N$_3$, [^{99m}Tc(N$_3$)(CDO)(CDOH)$_2$B-IS]; ^{99m}Tc-MPboroxime, [^{99m}TcCl(CDO)(CDOH)$_2$B-MP] (MP = *N*-methylpyridinium-4-yl); ^{99m}Tc-MPboroxime-N$_3$, [^{99m}Tc(N$_3$)(CDO)(CDOH)$_2$B-MP]; ^{99m}Tc-PAboroxime, [^{99m}TcCl(CDO)(CDOH)$_2$B(1*H*-pyrazol-3-yl)] (PA = 1*H*-pyrazol-3-yl); ^{99m}Tc-PAboroxime-N$_3$, [^{99m}Tc(N$_3$)(CDO)(CDOH)$_2$B-PA]; ^{99m}Tc-PYboroxime, [^{99m}TcCl(CDO)(CDOH)$_2$B(pyridin-3-yl)] (PY = pyridin-3-yl); ^{99m}Tc-PYboroxime-N$_3$, [^{99m}Tc(N$_3$)(CDO)(CDOH)$_2$B-pyridin-3-yl]; ^{99m}Tc-Sestamibi, [^{99m}Tc(MIBI)$_6$]$^+$ (MIBI = 2-methoxy-2-methylpropylisonitrile); ^{99m}Tc-Teboroxime, [^{99m}TcCl(CDO)(CDOH)$_2$-B-Me]; ^{99m}Tc-Teboroxime-N$_3$, [^{99m}Tc(N$_3$)(CDO)(CDOH)$_2$B-Me]; ^{99m}Tc-Trioxime, [^{99m}TcCl(CDO)(CDOH$_2$)$_2$]; ^{99m}Tc-Trioxime-N$_3$, [^{99m}Tc(N$_3$)(CDO)(CDOH$_2$)$_2$]; ^{99m}Tc-Uboroxime, [^{99m}TcCl(CDO)(CDOH)$_2$B-5U] (5U = uracil-5-yl); ^{99m}Tc-Uboroxime-N$_3$, [^{99m}Tc(N$_3$)(CDO)(CDOH)$_2$B-5U].

* Corresponding author at: School of Health Sciences, Purdue University, 550 Stadium Mall Drive, West Lafayette, IN, 47907, USA. Tel.: +1 765 494 0236; fax: +1 765 496 1377.
E-mail address: liu100@purdue.edu (S. Liu).

http://dx.doi.org/10.1016/j.nucmedbio.2016.05.001
0969-8051/

severity of disease, assessing the myocardial viability, establishing the need for surgical intervention, and monitoring the effects of treatment in CAD patients [7–10].

^{99m}Tc-Sestamibi is the most widely used radiotracer in nuclear cardiology over the last 30 years. A significant drawback of ^{99m}Tc-Sestamibi is its low first-pass extraction fraction and lack of linear relationship between heart uptake and regional blood flow at >2.5 mL/min/g [3–7]. In contrast, ^{99m}Tc-Teboroxime has the highest first-pass extraction fraction among all ^{99m}Tc perfusion radiotracers [7–20]. The linear relationship between its heart uptake and blood flow permits accurate detection of CAD and precise delineation of perfusion defects [7–10,13–17]. However, clinical experiences were disappointing due to its short myocardial retention [12–16]. The heart washout is too fast for standard SPECT cameras to acquire high-quality heart images. With recent developments in CZT-based cardiac SPECT cameras (e.g. D-SPECT from Spectrum Dynamics, IQ SPECT® developed by Siemens Medical Solutions and CardiArc® manufactured by CardiArc Inc.) over the last several years [6,21–29], the leaders in nuclear cardiology have been repeatedly calling for more efficient perfusion radiotracers with longer myocardial retention and improved biodistribution properties [9,29–32].

We have been interested in cationic and neutral ^{99m}Tc complexes as heart imaging agents [33–45]. Recently, we reported ^{99m}Tc(III) complexes [^{99m}TcCl(CDO)(CDOH)$_2$B-R] (Fig. 1: ^{99m}Tc-ISboroxime: R = IS; ^{99m}Tc-MPboroxime: R = MP; ^{99m}Tc-PAboroxime: R = PA; ^{99m}Tc-PYboroxime: R = PY; and ^{99m}Tc-Uboroxime: R = 5U) as radiotracers for heart imaging [45]. The results from biodistribution and imaging studies showed that ^{99m}Tc-PAboroxime had the heart uptake comparable to that of ^{99m}Tc-Teboroxime, but it had much longer myocardial retention time [45]. We also found that ^{99m}Tc-Teboroxime-N_3 had longer heart retention time than ^{99m}Tc-Teboroxime [44]. These promising results lead us to prepare complexes [^{99m}Tc(N_3)(CDO)(CDOH)$_2$B-R] (Fig. 1: ^{99m}Tc-ISboroxime-N_3, ^{99m}Tc-MPboroxime-N_3, ^{99m}Tc-PAboroxime-N_3, ^{99m}Tc-PYboroxime-N_3, and ^{99m}Tc-Uboroxime-N_3).

As an extension of our continuing efforts, we now present the syntheses and preliminary evaluations of complexes [^{99m}Tc(N_3)(CDO)(CDOH)$_2$B-R] for their potential as heart imaging agents. We kept the $CDOH_2$-core in order to maintain the high initial heart uptake for ^{99m}Tc(III) complexes [^{99m}Tc(N_3)(CDO)(CDOH)$_2$B-R]. The azide coligand is of our particular interest because ^{99m}Tc-Teboroxime-N_3 has a longer myocardial retention than ^{99m}Tc-Teboroxime [44]. The main objective of this study is to explore the impact of azide coligand and boronate caps on biodistribution properties (initial heart uptake and myocardial retention times) of ^{99m}Tc(III)-azide complexes [^{99m}Tc(N_3)(CDO)(CDOH)$_2$B-R]. Our ultimate goal is to develop a new ^{99m}Tc radiotracer that has longer myocardial retention than that of ^{99m}Tc-Terboroxime while maintaining the high initial heart uptake and high first-pass extraction fraction. A more stable heart uptake and longer myocardial retention will help to maintain the initial linear relationship between the radiotracer uptake and regional blood flow [18].

2. Experimental methods

2.1. Materials

Chemicals (citric acid, γ-cyclodextrin, cyclohexanedione dioxime (CDOH), diethylenetriaminepentaacetic acid (DTPA), isoxazole-4-boronic acid (IS), 1*H*-pyrazol-3-ylboronic acid (PA), 3-pyridineboronic acid (PY), *N*-methylpyridinium-4-boronic acid iodide (MP), sodium chloride, stannous chloride dihydrate, and uracil-5-boronic acid (5U)) were purchased from Sigma/Aldrich (St. Louis, MO), and were used without further purification. Na^{99m}TcO$_4$ was obtained from Cardinal HealthCare® (Indianapolis, IN).

2.2. Radio-HPLC method

The radio-HPLC method for routine analysis of ^{99m}Tc(III)-azide complexes [^{99m}Tc(N_3)(CDO)(CDOH)$_2$B-R] (R = IS, MP, PA, PY and 5U) used an Agilent HP-1100 HPLC system (Agilent Technologies, Santa Clara, CA) equipped with a β-ram IN/US detector (Tampa, FL) and Zorbax C_8 column (4.6 mm × 250 mm, 300 Å pore size; Agilent Technologies, Santa Clara, CA). The flow rate was 1 mL/min. The mobile phase was isocratic between 0 and 5 min with 30% solvent A (10 mM NH_4OAc buffer, pH = 6.8) and 70% solvent B (methanol), followed by a gradient from 70% solvent B at 5 min to and 90% solvent B at 20 min. The radiochemical purity (RCP) was reported as the percentage of area for the expected radiometric peak on each radio-HPLC chromatogram of

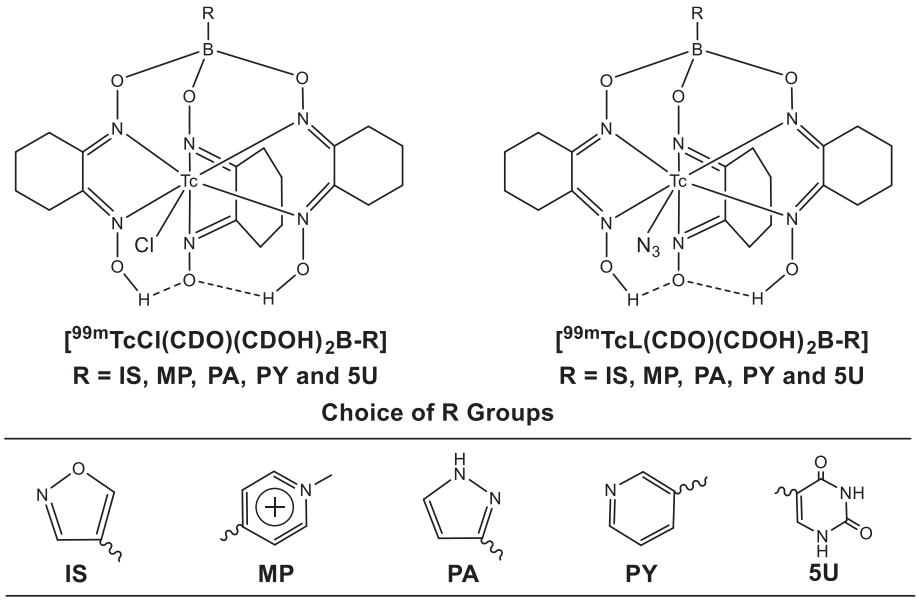

Fig. 1. Chemdraw structures of ^{99m}Tc(III) complexes [^{99m}TcCl(CDO)(CDOH)$_2$B-R] (Left: ^{99m}Tc-ISboroxime: R = IS; ^{99m}Tc-MPboroxime: R = MP; ^{99m}Tc-PAboroxime: R = PA; ^{99m}Tc-PYboroxime: R = PY; and ^{99m}Tc-Uboroxime: R = 5U), and new ^{99m}Tc(III)-azide complexes [^{99m}Tc(N_3)(CDO)(CDOH)$_2$B-R] (^{99m}Tc-ISboroxime-N_3: R = IS; ^{99m}Tc-MPboroxime-N_3: R = MP; ^{99m}Tc-PAboroxime-N_3: R = PA; ^{99m}Tc-PYboroxime-N_3: R = PY; and ^{99m}Tc-Uboroxime-N_3: R = 5U) evaluated as heart imaging agents in this study. Structures of complexes [^{99m}TcCl(CDO)(CDOH)$_2$B-R] were derived from those of complexes [ReCl(CDO)(CDOH)$_2$BPh], [TcX(dioxime)$_3$B-R] (X = Cl, Br; dioxime = dimethylglyoxime, cyclohexanedione dioxime; R = CH_3 and C_4H_9) and [Tc(NCS) (CDO) (CDOH)$_2$BMe] [46–48].

each ^{99m}Tc(III) radiotracer. The ITLC method used Gelman Sciences silica-gel strips and a 1:1 (v:v) mixture of acetone and saline as the mobile phase. ^{99m}Tc radiotracers and $^{99m}TcO_4^-$ migrated to solvent front while [^{99m}Tc]colloid stayed at the origin.

2.3. Preparation of [^{99m}Tc(N_3)(CDO)$(CDOH)_2$B-R] (R = IS, MP, PA, PY and 5U)

All ^{99m}Tc(III) radiotracers were prepared using the kit formulation [44,45]. Each lyophilized vial contains 2 mg of $CDOH_2$, 4–5 mg of boronic acid, 50–60 μg of $SnCl_2{\circ}2H_2O$, 9 mg of citric acid, 2 mg of DTPA and 20 mg of NaCl and 10 mg of γ-cyclodextrin. To a lyophilized vial was added 1.0 mL $^{99m}TcO_4^-$ solution (370–1110 MBq) in saline. The reconstituted vial was then heated at 100 °C for 10–15 min. After addition of NaN_3 (4–5 mg dissolved in 0.2 mL saline), the vial was heated at 100 °C for another 10–15 min. A sample of the resulting solution was diluted with saline containing ~20% propylene glycol. The diluted solution was analyzed by HPLC and ITLC. The RCP was 80–98% with minimum of [^{99m}Tc]colloid (<0.5%). The RCP must be >90% for biodistribution and imaging studies of new ^{99m}Tc radiotracers. Their solution stability was monitored by radio-HPLC at 0, 2, 4, and 6 h post-labeling.

2.4. Doses preparation

Doses for biodistribution were prepared by dissolving radiotracer to ~1.1 MBq/mL with saline containing 20% propylene glycol. Doses for imaging studies were made by dissolving the radiotracer to ~370 MBq/mL with saline containing 20% propylene glycol. All dose solutions were filtered with a 0.20 μm filter unit to eliminate foreign particles and make the injectate sterile before being injected into animals. The injection volume was ~0.1 mL per animal for biodistribution and 0.2–0.5 mL per animal for imaging studies.

2.5. Animal preparation

Animal studies were conducted in compliance with the NIH animal experiment guidelines (*Principles of Laboratory Animal Care*, NIH Publication No. 86-23, revised 1985). The protocols for biodistribution and imaging studies were approved by the Purdue University Animal Care and Use Committee (PACUC). The SD rats (200–250 g) were purchased from Harlan (Indianapolis, IN), and were acclimated for more than 24 h. Animals were anesthetized with intramuscular injection of a mixture of ketamine (80 mg/kg) and xylazine (19 mg/kg) before being used for biodistribution and planar imaging studies.

2.6. Protocol for biodistribution

Twelve SD rats (200–250 g) were divided randomly into three groups. Each animal was administered with 100–111 KBq of ^{99m}Tc radiotracer via the tail vein injection. Four animals were sacrificed by sodium pentobarbital overdose (100–200 mg/kg) at 2, 15 and 30 min p.i. Blood was withdrawn directly from the heart. Organs of interest (heart, brain, intestines, kidneys, liver, lungs, muscle, and spleen) were harvested, rinsed with saline, dried with absorbent tissues, weighed and counted for total radioactivity accumulation on a Perkin Elmer Wizard — 1480 γ-counter (Shelton, CT). The organ uptake was reported as the percentage of injected dose (%ID/organ) or the percentage of injected dose per gram of wet mass (%ID/g). Comparison between two radiotracers was made using one-way ANOVA test (GraphPad Prism 5.0, San Diego, CA). The level of significance was set at $p < 0.05$.

2.7. Protocol for dynamic planar imaging

Dynamic planar imaging studies were performed in SD rats (200–250 g). Five animals were used for each radiotracer. Each animal was administered with ^{99m}Tc radiotracer (40–80 MBq) through the tail vein injection. Once the ^{99m}Tc radiotracer was administered, the animal was immediately placed prone on a single head mini γ-camera (Diagnostic Services Inc., NJ). The 1-min static images were acquired during first 5 min p.i., followed by the 2-min static images at 6–30, 40, 50 and 60 min p.i. The planar imaging data were stored digitally in a 128 × 128 matrix. After imaging, animals were returned to a lead-shielded cage to recover. Since all new radiotracers virtually had no excretion via hepatobiliary and renal routes, the planar images were analyzed by drawing regions of the heart (the heart radioactivity) and whole body (the total radioactivity injected into each animal). The background activity was corrected by drawing the region right above the heart. The results were expressed as the percentage of injected radioactivity (%ID). The exponential fit of heart retention was determined using GraphPad Prism 5.0 (GraphPad Software, Inc., San Diego, CA).

2.8. Protocol for SPECT

SPECT study was performed the u-SPECT-II/CT scanner (Milabs, Utrecht, The Netherlands) equipped with a 1.0 mm multi-pinhole collimator. The SD rat was placed into a shielded chamber connected to an isoflurane anesthesia unit (Univentor, Zejtun, Malta). Anesthesia was induced using an air flow rate of 350 mL/min and ~3.0% isoflurane, and maintained using an air flow of ~250 mL/min with ~2.5% isoflurane during image data acquisition (6 frames: 75 projections over 5 min per frame). ^{99m}Tc-ISboroxime-N_3 (~185 MBq dissolved in 0.5 mL saline containing ~20% propylene glycol) was injected into the animal via tail vein through a catheter, followed with 0.5 mL saline solution flash. Rectangular scan in regions of interest (ROIs) from SPECT and CT were selected one the basis of orthogonal X-ray images provided by CT. After SPECT acquisition, the animal was allowed to recover in a cage.

2.9. Image reconstruction and data processing

SPECT reconstruction was performed using a POSEM (pixelated ordered subsets by expectation maximization) algorithm with 6 iterations and 16 subsets. CT data were reconstructed using a cone-beam filtered back-projection algorithm (NRecon v1.6.3, Skyscan). After reconstruction, the SPECT and CT data were automatically co-registered according to the movement of the robotic stage, and re-sampled to equivalent voxel sizes. Co-registered images were further rendered and visualized using the PMOD software (PMOD Technologies, Zurich, Switzerland). A 3D-Guassian filter (1.2 mm FWHM) was applied to smooth noise, and the LUTs (look up tables) were adjusted for good visual contrast. The images were visualized as both orthogonal slices and maximum intensity projections.

3. Results

3.1. Radiochemistry

New complexes [^{99m}Tc(N_3)$(CDOH)_2$B-R] (R = IS, MP, PA, PY and 5U) were prepared according to Chart I. First, complexes [^{99m}TcCl(CDO)$(CDOH)_2$B-R] (R = IS, MP, PA, PY and 5U) were prepared using the literature method [11,44,45], and then were allowed to react with NaN_3. Heating at 100 °C was needed to complete the Cl-N_3 ligand exchange because their RCP was <5% when the reaction was performed at room temperature. ^{99m}Tc-ISboroxime-N_3, ^{99m}Tc-PYboroxime-N_3 and ^{99m}Tc-Uboroxime-N_3 were prepared with the RCP being >93%. In contrast, the RCP for ^{99m}Tc-MPboroxime-N_3 and ^{99m}Tc-PAboroxime-N_3 was only 80–85% despite our efforts to improve their RCP by altering component levels in each vial or changing the radiolabeling conditions. All new ^{99m}Tc(III)-azide complexes [^{99m}Tc(N_3)$(CDOH)_2$B-R] (R = IS, MP, PA, PY and 5U) were stable in solution for >6 h post-labeling (data not shown), and had higher lipophilicity than their corresponding ^{99m}Tc(III)-chloride complexes [^{99m}TcCl$(CDOH)_2$B-R] (R = IS, MP, PA,

PY and 5U), as indicated by their significantly longer HPLC retention times (Table 1).

The main radio-impurity was the radiometric peak at ~7 min in radio-HPLC chromatograms of ^{99m}Tc(III) complexes [^{99m}Tc(N_3)(CDO)$(CDOH)_2$B-R] (R = IS, MP and PA) (Fig. 2), likely from the ^{99m}Tc(III)-species without the boronate cap. To prove this hypothesis, we prepared complexes [^{99m}TcCl(CDO)$(CDOH_2)_2$] (^{99m}Tc-Trioxime) and [^{99m}Tc(N_3)(CDO)$(CDOH_2)_2$] (^{99m}Tc-Trioxime-N_3) without using boronic acid. Fig. 3 shows radio-HPLC chromatograms of ^{99m}Tc-Trioxime and ^{99m}Tc-Trioxime-N_3. The HPLC retention time of ^{99m}Tc-Trioxime-N_3 matches perfectly with the 7-min peak observed in the radio-HPLC chromatograms (Fig. 2) of complexes [^{99m}Tc(N_3)(CDO)$(CDOH)_2$B-R] (R = IS, MP and PA).

3.2. Dynamic planar imaging

Dynamic planar imaging is an important tool to evaluate the heart washout kinetics of new ^{99m}Tc radiotracers without sacrificing a large number of animals. By semi-quantification of planar images, it is possible to estimate the heart uptake expressed as the percentage of injected dose (%ID). However, it is much more difficulty to do the same for liver radioactivity due to its larger size and difficulty to identify the boundary between liver and other organs in the same region. Therefore, planar dynamic imaging studies focused on the initial heart uptake and heart retention times of ^{99m}Tc-ISboroxime-N_3, ^{99m}Tc-PYboroxime-N_3 and ^{99m}Tc-Uboroxime-N_3. We excluded ^{99m}Tc-MPboroxime-N_3 and ^{99m}Tc-PAboroxime-N_3 from these studies because of their low RCP (<90%). The presence of radio-impurities makes it difficult to accurately quantify the heart uptake at a specific time and to interpret the experimental results from planar imaging studies. Fig. 4 displays planar images of the SD rats after administration of ^{99m}Tc-ISboroxime-N_3, ^{99m}Tc-PYboroxime-N_3 and ^{99m}Tc-Uboroxime-N_3. Image quantification data were summarized in Fig. 5 to compare their initial heart uptake (%ID) and myocardial retention times, expressed as the fast phase half-life. The heart retention curves were best fitted to a bi-exponential function all three new radiotracers.

All new radiotracers shared very similar heart clearance kinetics with ^{99m}Tc-Teboroxime (Fig. 5). The initial heart uptake of ^{99m}Tc-ISboroxime-N_3 (5.5 ± 0.4%ID) and ^{99m}Tc-PYboroxime-N_3 (4.7 ± 0.7%ID) was comparable to that reported for ^{99m}Tc-Teboroxime (5.6 ± 0.7%ID), ^{99m}Tc-ISboroxime (5.0 ± 1.1%ID) and ^{99m}Tc-PYboroxime (4.1 ± 0.8%ID), respectively, within the experimental errors [44,45]. The initial heart uptake of ^{99m}Tc-Uboroxime-N_3 (4.6 ± 0.9%ID) was higher ($p < 0.05$) than that for ^{99m}Tc-Uboroxime (3.2 ± 0.7%ID) [45]. Its myocardial retention time (0.9 ± 0.4 min) was also longer than that for ^{99m}Tc-Uboroxime (0.3 ± 0.1 min) [45], suggesting that the use of azide coligand increases the heart uptake and myocardial retention time of ^{99m}Tc(III) radiotracer. However, this effect is not always same for different ^{99m}Tc(III) radiotracers. The myocardial retention time followed the ranking order of ^{99m}Tc-ISboroxime-N_3 (1.6 ± 0.4 min) ~ ^{99m}Tc-Teboroxime (1.7 ± 0.8 min) > ^{99m}Tc-Uboroxime-N_3 (0.9 ± 0.4 min) ~ ^{99m}Tc-PYboroxime-N_3 (0.7 ± 0.1 min).

Table 1
Radiochemical purity data and HPLC retention times of ^{99m}Tc(III)-azide complexes [^{99m}TcL(CDO)$(CDOH)_2$B-R] (L = Cl and N_3; R = Me, IS, MP, PA, PY and 5U).

Radiotracer	HPLC Retention Time (min)	Radiochemical Purity (%)
^{99m}Tc-Teboroxime[a]	15.5	>95%
^{99m}Tc-Teboroxime-N_3	18.3	>95%
^{99m}Tc-ISboroxime[b]	11.2	>93%
^{99m}Tc-ISboroxime-N_3	15.2	>95%
^{99m}Tc-MPboroxime[b]	9.3	90–95%
^{99m}Tc-MPboroxime-N_3	14.5	80–85%
^{99m}Tc-PAboroxime[b]	9.5	90–95%
^{99m}Tc-PAboroxime-N_3	14.5	80–85%
^{99m}Tc-PYboroxime[b]	13.7	>95%
^{99m}Tc-PYboroxime-N_3	18.7	>95%
^{99m}Tc-Uboroxime[b]	10.5	>95%
^{99m}Tc-Uboroxime-N_3	15.5	90–95%
^{99m}Tc-Trioxime	4.4	>95%
^{99m}Tc-Trioxime-N_3	7.2	>95%

[a] Data from Ref. [46].
[b] Data from Ref. [47].

3.3. Biodistribution properties

We used the 2-min heart uptake data as another screening tool to evaluate new radiotracers. The selected 2-min biodistribution data of ^{99m}Tc-PYboroxime-N_3, ^{99m}Tc-Uboroxime-N_3 and ^{99m}Tc-Trioxime in SD rats are summarized in Table 2. We obtained the 2-min biodistribution data for ^{99m}Tc-Trioxime to illustrate the impact of radio-impurity. Table 3 lists the biodistribution data of ^{99m}Tc-ISboroxime-N_3 at 2, 15 and 30 min p.i. Fig. 6 compares their 2-min heart uptake of ^{99m}Tc-ISboroxime-N_3, ^{99m}Tc-PYboroxime-N_3, ^{99m}Tc-Uboroxime-N_3 and ^{99m}Tc-Trioxime with those for ^{99m}Tc-Teboroxime and ^{99m}Tc-Sestamibi [44]. We found that the 2-min heart uptake followed the general ranking order of ^{99m}Tc-ISboroxime-N_3 (3.60 ± 0.28%ID/g) ≥ ^{99m}Tc-Teboroxime (3.00 ± 0.37%ID/g) > ^{99m}Tc-Sestamibi (2.56 ± 0.31%ID/g) ≥ ^{99m}Tc-PYboroxime-N_3 (2.35 ± 0.37%ID/g) > ^{99m}Tc-Trioxime (1.75 ±0.07%ID/g) ≫ ^{99m}Tc-Uboroxime-N_3 (1.29 ± 0.06%ID/g). ^{99m}Tc-ISboroxime-N_3 had the highest 2-min heart uptake among all ^{99m}Tc radiotracers revaluated in SD rats. These results were also consistent with the general trend observed in dynamic planar imaging studies (Fig. 5).

We were particularly interested in ^{99m}Tc-ISboroxime-N_3 for full-scale biodistribution study due to its high initial heart uptake (Fig. 5). ^{99m}Tc-PYboroxime-N_3 and ^{99m}Tc-Uboroxime-N_3 were excluded because of their much faster heart washout (Fig. 5). We found that the 2-min heart uptake of ^{99m}Tc-ISboroxime-N_3 (3.60 ± 0.28%ID/g) was almost identical to that reported for ^{99m}Tc-ISboroxime (3.75 ± 0.68%ID/g) [45]. However, ^{99m}Tc-ISboroxime-N_3 (1.06 ± 0.18 and 0.62 ± 0.09%ID/g 15 and 30 min p.i., respectively) had a lower heart uptake at later time points than ^{99m}Tc-ISboroxime (1.68 ± 0.69 and 1.33 ± 0.34%ID/g 15 and 30 min p.i., respectively). The heart washout kinetics of ^{99m}Tc-ISboroxime-N_3 was very similar to that of ^{99m}Tc-Teboroxime (heart uptake: 3.00 ± 0.37, 1.25 ± 0.09 and 0.86 ± 0.17%ID/g at 2, 15 and 30 min p.i., respectively). The blood radioactivity level of ^{99m}Tc-ISboroxime-N_3 (0.31 ± 0.04, 0.21 ± 0.01 and 0.16 ± 0.01%ID/g at 2, 15 and 30 min

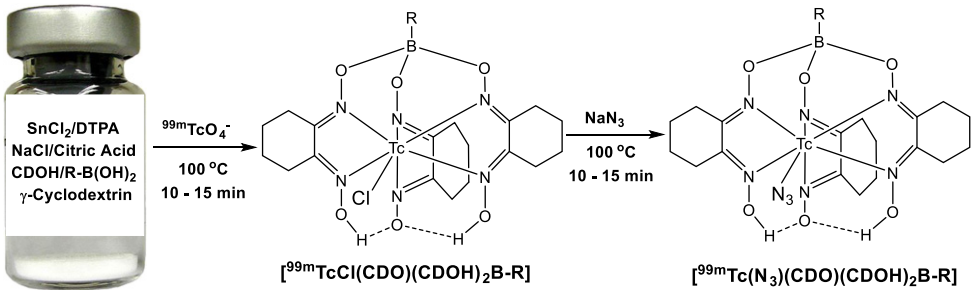

Chart I. Synthesis of Complexes [^{99m}Tc(N_3)(CDO)$(CDOH)_2$B-R] (R = IS, MP, PA, PY and 5U).

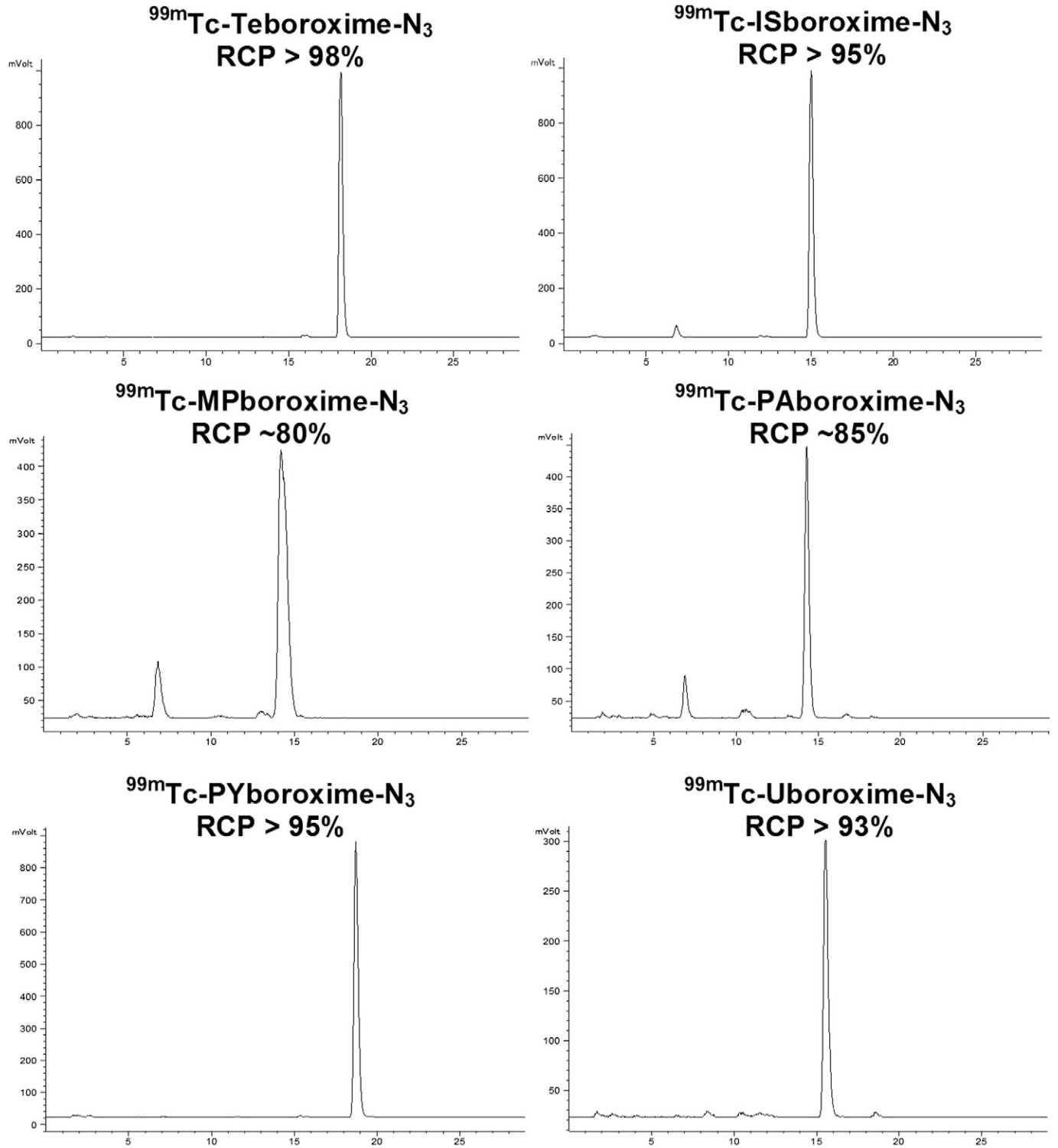

Fig. 2. HPLC chromatograms for ^{99m}Tc-Teboroxime-N_3 (RCP > 98%), ^{99m}Tc-ISboroxime-N_3 (RCP > 95%), ^{99m}Tc-MPboroxime-N_3 (RCP ~ 80%), ^{99m}Tc-PAboroxime-N_3 (RCP ~ 85%), ^{99m}Tc-PYboroxime-N_3 (RCP > 98%) and ^{99m}Tc-Uboroxime-N_3 (RCP > 93%). The radiometric peak at ~7 min is from a ^{99m}Tc-species without boronate-capping group. ^{99m}Tc-Teboroxime(N_3) was used for comparison purpose.

p.i., respectively) was lower than that for ^{99m}Tc-ISboroxime (0.54 ± 0.20, 0.35 ± 0.10 and 0.39 ± 0.08%ID/g at 2, 15 and 30 min p.i., respectively) over the same study period [45]. The lung uptake of ^{99m}Tc-ISboroxime-N_3 (1.08 ± 0.32, 0.83 ± 0.06 and 0.70 ±0.14%ID/g at 2, 15 and 30 min p.i., respectively) was also lower ($p < 0.05$) than that of ^{99m}Tc-ISboroxime (2.34 ± 0.93, 1.27 ± 0.33 and 1.59 ± 0.76%ID/g at 2, 15 and 30 min p.i., respectively) and ^{99m}Tc-Teboroxime (2.90 ± 0.35, 1.64 ± 0.28 and 1.41 ± 0.25 and 0.94 ±0.25%ID/g at 2, 15 and 30 min p.i., respectively). Even though ^{99m}Tc-ISboroxime-N_3 (4.42 ± 0.38%ID/g) had higher 2-min liver uptake than ^{99m}Tc-ISboroxime (3.24 ± 0.55%ID/g), its liver clearance was faster (Table 2). The blood vessel activity for ^{99m}Tc-ISboroxime-N_3

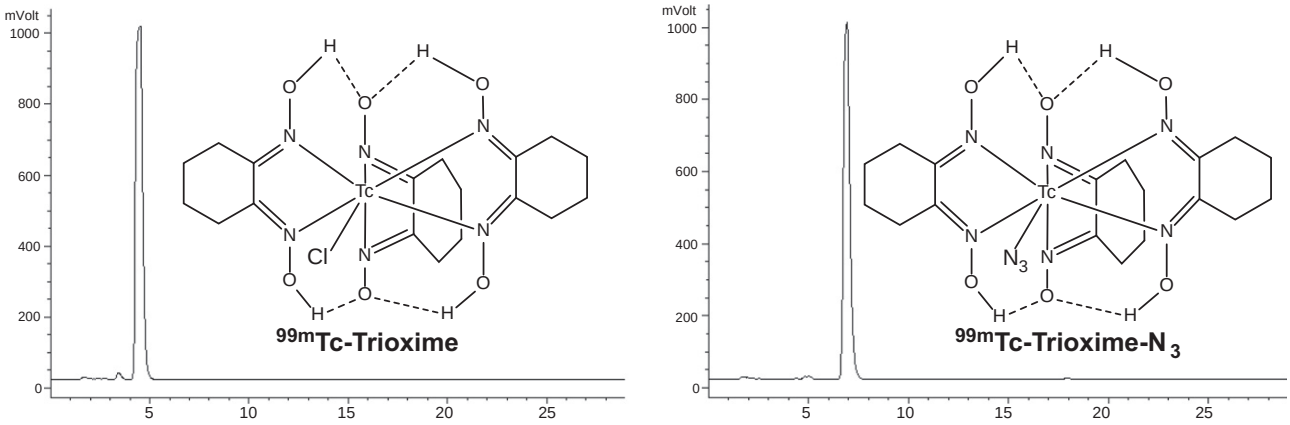

Fig. 3. Typical HPLC chromatograms of ^{99m}Tc-Trioxime and ^{99m}Tc-Trioxime-N_3. Their RCP was >98%. The retention time of ^{99m}Tc-Trioxime-N_3 matches well with that of the radiometric peak observed in the HPLC chromatograms of ^{99m}Tc-ISboroxime-N_3, ^{99m}Tc-MPboroxime-N_3 and ^{99m}Tc-PAboroxime-N_3 (Fig. 2).

(0.47 ±0.05%ID/g) at 2 min p.i. was lower than that for ^{99m}Tc-ISboroxime-N_3 (1.92 ± 0.19%ID/g) [45]. However, they had almost identical blood vessel radioactivity levels at 15 and 30 min p.i.

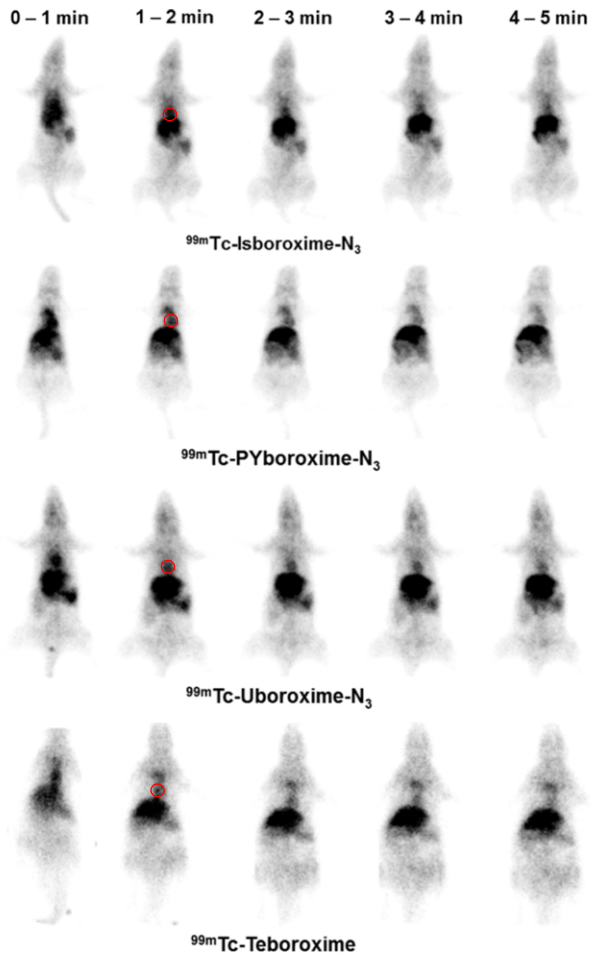

Fig. 4. The whole-body planar images of the SD rats administered with ^{99m}Tc-ISboroxime-N_3, ^{99m}Tc-PYboroxime-N_3 or ^{99m}Tc-Uboroxime-N_3 over the first 5 min p.i. ^{99m}Tc-Teboroxime were used for comparison purpose. Animals were anesthetized with intramuscular injection of a mixture of ketamine (80 mg/kg) and xylazine (19 mg/kg). Each animal was administered with 1.0–1.5 mCi of ^{99m}Tc radiotracer. Red circles indicate the presence of heart radioactivity.

3.4. SPECT imaging

A SPECT study was performed with ^{99m}Tc-ISboroxime-N_3 due to its high initial heart uptake (Table 2). Fig. 7A illustrates SPECT images of the SD rat administered with ^{99m}Tc-ISboroxime-N_3. High quality SPECT images were acquired despite its high liver uptake. The right and left ventricular walls were clearly delineated. The interference from liver radioactivity in coronal and sagittal images was not significant over the 30-min period. However, the liver radioactivity overlapped significantly with that in the inferior wall of the heart in the transaxial images. The best image acquisition window is 0–5 min for ^{99m}Tc-ISboroxime-N_3 (Fig. 7A). Longer acquisition time did not improve the image quality be-

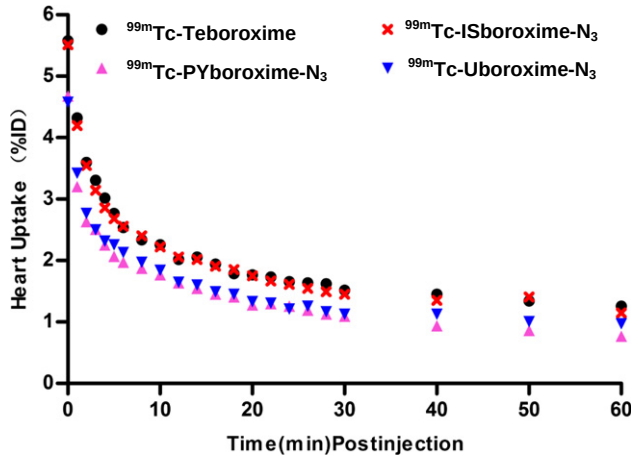

Radiotracer	Initial Heart Uptake (%ID)	Fast Phase Half-life (min)
^{99m}Tc-ISboroxime(N_3)	5.5±0.3	1.6±0.4
^{99m}Tc-PYboroxime(N_3)	4.±0.77	0.7±0.1
^{99m}Tc-Uboroxime(N_3)	4.6±0.9	0.9±0.4
^{99m}Tc-Teboroxime	5.6±0.7	1.7±0.8

Fig. 5. Image quantification data to compare the initial heart uptake and heart retention times of ^{99m}Tc(III)-azide complexes [^{99m}Tc(N_3)(CDO)(CDOH)$_2$B-R] (R = IS, PY and 5U) over the first 5 min. ^{99m}Tc-Teboroxime was used purely for comparison purpose. All experimental data in this figure were derived from planar images. The initial heart uptake was expressed as the %ID at 0–1 min p.i. The curve lines and standard error bars were omitted for the purpose of clarity.

Table 2
The 2-min biodistribution data and heart-to-background ratios for ^{99m}Tc-PYboroxime-N_3, ^{99m}Tc-Uboroxime-N_3 and ^{99m}Tc-Trioxime in SD rats.

Radiotracer	^{99m}Tc-PYboroxime-N_3 (%ID/g)	^{99m}Tc-Uboroxime-N_3 (%ID/g)	^{99m}Tc-Trioxime (%ID/g)
Blood	0.25 ± 0.03	0.63 ± 0.09	0.50 ± 0.06
Brain	0.07 ± 0.01	0.02 ± 0.00	0.02 ± 0.00
Heart	2.35 ± 0.37	1.29 ± 0.06	1.75 ± 0.07
Intestines	0.77 ± 0.19	0.97 ± 0.16	1.04 ± 0.03
Kidneys	2.82 ± 0.46	3.32 ± 0.50	2.70 ± 0.29
Liver	3.73 ± 0.53	5.87 ± 1.09	3.23 ± 0.23
Lungs	1.31 ± 0.38	1.23 ± 0.11	0.78 ± 0.05
Muscle	0.16 ± 0.02	0.16 ± 0.04	0.21 ± 0.04
Spleen	1.55 ± 0.28	1.02 ± 0.60	0.93 ± 0.08
Vessels	0.94 ± 0.73	0.43 ± 0.05	0.67 ± 0.18
Heart/Blood	9.54 ± 0.75	2.07 ± 0.30	3.56 ± 0.56
Heart/Liver	0.65 ± 0.14	0.23 ± 0.06	0.55 ± 0.06
Heart/Lung	1.85 ± 0.21	1.06 ± 0.13	2.25 ± 0.06
Heart/Muscle	14.64 ± 3.17	8.58 ± 2.40	8.83 ± 1.57

cause of its fast myocardial washout (Fig. 7B) and the prolonged liver radioactivity accumulation (Fig. 4). The heart radioactivity washout was too fast to acquire high quality SPECT images at >5 min p.i. Similar results were obtained with ^{99m}Tc-Teboroxime (Fig. 7B).

4. Discussion

In this study, we evaluated five ^{99m}Tc(III)-azide complexes [^{99m}Tc(N_3)(CDO)$(CDOH)_2$B-R] (R = IS, MP, PA, PY and 5U) for their potential as heart imaging agents. ^{99m}Tc-MPboroxime-N_3 and ^{99m}Tc-PAboroxime-N_3 had relatively low RCP (80–85%) while the RCP was >93% for ^{99m}Tc-ISboroxime-N_3, ^{99m}Tc-PYboroxime-N_3 and ^{99m}Tc-Uboroxime-N_3. Since all complexes [^{99m}Tc(N_3)(CDO)$(CDOH)_2$B-R] (R = IS, MP, PA, PY and 5U) had longer HPLC retention times than complexes [^{99m}TcCl(CDO)$(CDOH)_2$B-R] (R = IS, MP, PA, PY and 5U) (Table 1), it is reasonable to believe that the chloride ligand in [^{99m}TcCl(CDO)$(CDOH)_2$B-R] is replaced by the N_3^- ligand. This statement is consistent with the fact that completion of the Cl-N_3 ligand exchange requires 100 °C heating for 10–15 min. Structures of complexes [ReCl(CDO)$(CDOH)_2$BPh] and [TcX(dioxime)$_3$B-R] (X = Cl, Br; dioxime = dimethylglyoxime, cyclohexanedione dioxime; R = CH_3 and C_4H_9) have been reported in the literature [46,47]. The structures of complexes [^{99m}Tc(N_3)(CDO)$(CDOH)_2$B-R] (R = IS, MP, PA, PY and 5U) are not known. The structural characterization of complexes [M(N_3)(CDO)$(CDOH)_2$B-R] (M = Tc and Re) is difficult because organic azides and heavy metal azide salts tend to be highly heat and shock-sensitive explosives (https://en.wikipedia.org/wiki/Azide). Due to the similarity (isoelectronic) between SCN^- and N_3^-, it is reasonable to believe that complexes [^{99m}Tc(N_3)(CDO)$(CDOH)_2$B-R] would share very similar structures with those of [M(NCS)(CDO)$(CDOH)_2$B-Me] (M = Tc and Re), which have been determined by X-ray crystallography [48]. This assumption is completely consistent with the fact that ^{99m}Tc-Teboroxime-NCS and ^{99m}Tc-Teboroxime-N_3 shared almost identical HPLC retention times of under the same chromatographic conditions [44].

Among the radiotracers evaluated in planar imaging studies, ^{99m}Tc-ISboroxime-N_3 has the highest initial heart uptake with the heart retention comparable to that of ^{99m}Tc-Teboroxime (Fig. 5). This observation was further substantiated by the biodistribution data (Table 2) and results from SPECT/CT studies (Fig. 7). The impact of azide coligand on the heart uptake and myocardial retention times depends on boronate caps. For example, ^{99m}Tc-ISboroxime-N_3 shares similar biodistribution properties with ^{99m}Tc-ISboroxime [45]. ^{99m}Tc-Uboroxime-N_3 (Fig. 5) has much higher initial heart uptake with longer myocardial retention than ^{99m}Tc-Uboroxime [45]. In contrast, ^{99m}Tc-PYboroxime-N_3 has

Table 3
Selected biodistribution data and heart-to-background ratios for ^{99m}Tc-ISboroxime-N_3 in SD rats.

Organ	2 min (n = 4) (%ID/g)	15 min (n = 4) (%ID/g)	30 min (n = 3) (%ID/g)
Blood	0.31 ± 0.04	0.21 ± 0.01	0.16 ± 0.01
Brain	0.12 ± 0.01	0.08 ± 0.01	0.06 ± 0.01
Heart	3.60 ± 0.28	1.06 ± 0.18	0.62 ± 0.09
Intestines	1.23 ± 0.41	1.78 ± 0.60	2.36 ± 1.31
Kidneys	2.81 ± 0.41	1.19 ± 0.06	0.90 ± 0.03
Liver	4.42 ± 0.38	2.33 ± 0.30	1.55 ± 0.25
Lungs	1.08 ± 0.32	0.83 ± 0.06	0.70 ± 0.14
Muscle	0.16 ± 0.02	0.27 ± 0.04	0.24 ± 0.03
Spleen	1.02 ± 0.60	0.64 ± 0.09	0.44 ± 0.05
Vessels	0.47 ± 0.05	1.02 ± 0.15	1.52 ± 0.62
Heart/Blood	14.63 ± 4.78	5.10 ± 0.83	4.00 ± 0.61
Heart/Liver	0.82 ± 0.11	0.45 ± 0.02	0.41 ± 0.06
Heart/Lung	4.42 ± 1.80	1.27 ± 0.13	0.92 ± 0.13
Heart/Muscle	26.90 ± 6.66	3.93 ± 0.49	2.57 ± 0.20

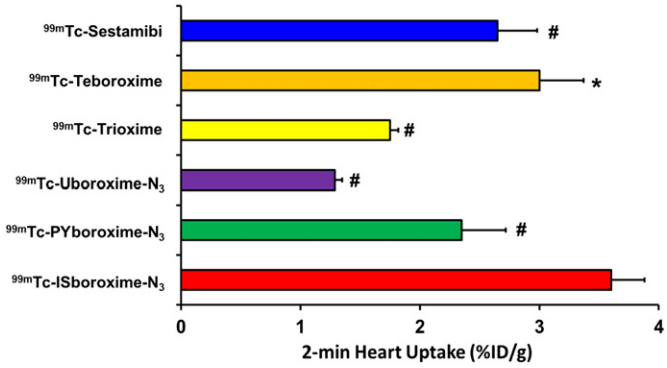

Fig. 6. Direct comparison of the 2-min heart uptake values (%ID/g) of ^{99m}Tc-ISboroxime-N_3, ^{99m}Tc-PYboroxime-N_3 and ^{99m}Tc-Uboroxime-N_3 with known radiotracers: ^{99m}Tc-Sestamibi and ^{99m}Tc-Teboroxime. #: $p < 0.01$ and *: $p < 0.05$ vs. ^{99m}Tc-ISboroxime-N_3. The 2-min heart uptake values for ^{99m}Tc-Sestamibi and ^{99m}Tc-Teboroxime were from our previous study [44]. The 2-min heart uptake of ^{99m}Tc-Trioxime was obtained for comparison purpose.

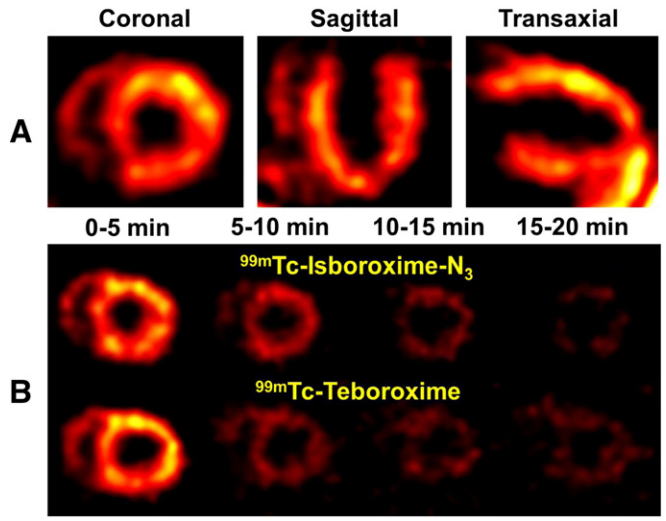

Fig. 7. A: Selected coronal, sagittal and transaxial views of SPECT images of the SD rat administered with ~80 MBq of ^{99m}Tc-ISboroxime-N_3 obtained at 0–5 min p.i. **B**: Coronal views of SPECT images of SD rats administered with 80–90 MBq of ^{99m}Tc-ISboroxime-N_3 and ^{99m}Tc-Teboroxime obtained at 0–5, 5–10, 10–15 and 15–20 min p.i. Animals were anesthetized with intramuscular injection of a mixture of ketamine (80 mg/kg) and xylazine (19 mg/kg). SPECT images were obtained over the first 5 min after its administration with camera being focused in the heart region. ^{99m}Tc-Teboroxime was used for comparison purpose. The best image acquisition window is 0–5 min for both radiotracers. The heart radioactivity washed out too fast to acquire high quality SPECT images at >5 min p.i.

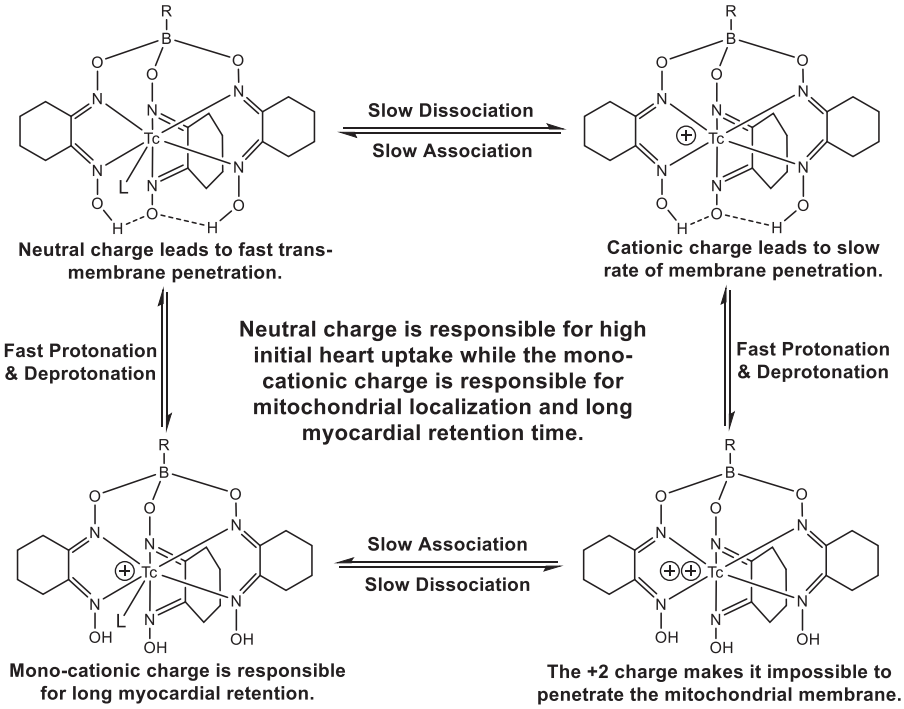

Chart II. Proposed Equilibrium between Different ^{99m}Tc(III) Complexes.

lower initial heart uptake and shorter myocardial retention time than ^{99m}Tc-PYboroxime [45]. It seems that this effect might be related the "increased lipophilicity" of ^{99m}Tc(III)-azide complexes. There is always a subtle balance between the lipophilicity, initial heart uptake and myocardial retention of radiotracers [37].

It was reported that the linear relationship between the heart uptake of ^{99m}Tc-Teboroxime and the regional blood flow is well maintained at 1–2 min after administration when the blood flow rates were 1–5 mL/m/g [18]. However, its heart uptake underestimates the flow changes at high or moderate flow rates >5 min after administration due to the "roll-off" phenomena, which leads to a progressive reduction in the slope of the uptake-flow relation and the loss of uptake-flow linearity at >2.5 mL/m/g [18]. That is why the 2-min biodistribution data were used to screen new ^{99m}Tc radiotracers. If the new ^{99m}Tc radiotracer has the 2-min heart uptake value very close to or better than that of ^{99m}Tc-Teboroxime, a full-scale biodistribution would be warranted. If the new ^{99m}Tc radiotracer has the 2-min heart uptake much less than that of ^{99m}Tc-Teboroxime, the full-scale biodistribution will not be worthy of further efforts, unless it is needed for comparison purposes. We found that this screening approach is quite cost-effective.

The heart uptake mechanism of ^{99m}Tc(III) complexes [^{99m}TcL(CDO)$(CDOH)_2$B-R] is not known. It has been suggested that [^{99m}Tc(H_2O)(CDO)$(CDOH)_2BCH_3]^+$ is responsible for the high heart uptake of ^{99m}Tc-Teboroxime [11]. This hypothesis seems consistent with the heart localization mechanism of many cationic ^{99m}Tc radiotracers [33–43,49–51]. However, it is not consistent with the fact that the ^{99m}Tc-azide complexes [^{99m}Tc(N_3)(CDO)$(CDOH)_2$B-R] have a high initial heart uptake with the myocardial retention comparable to or longer than that of their corresponding ^{99m}Tc-chloride complexes [^{99m}TcCl(CDO)$(CDOH)_2$B-R]. There must be an alternative mechanism for complexes [^{99m}TcL(CDO)$(CDOH)_2$B-R].

Based on experiences with cationic ^{99m}Tc radiotracers [33–43,49–51], we believe that the high initial uptake of [^{99m}TcL(CDO)$(CDOH)_2$B-R] might be related to the neutral charge while their myocardial retention is associated to their unique capability to form the equilibrium (Chart II) between [^{99m}TcL(CDO)$(CDOH)_2$B-R] and [^{99m}TcL$(CDOH)_3$B-R]$^+$. The neutral complex [^{99m}TcL(CDO)$(CDOH)_2$B-R] is able to across cellular and mitochondrial membranes with ease. The complex cation [^{99m}TcL$(CDOH)_3$B-R]$^+$ might be able to across the "leaky" cellular membrane, but it is much more difficult for [^{99m}TcL$(CDOH)_3$B-R]$^+$ to penetrate the highly packed rigid mitochondrial membranes. This may explain why the neutral radiotracers like ^{99m}Tc-Teboroxime tend to have higher first-pass extraction fraction than cationic ^{99m}Tc radiotracers, such as ^{99m}Tc-Sestamibi.

The conversion from [^{99m}TcL(CDO)$(CDOH)_2$B-R] to [^{99m}TcL$(CDOH)_3$B-R]$^+$ by protonation is easy (Chart II), particularly at lower pH. The same is true for the conversion (Chart II) between [^{99m}Tc(CDO)$(CDOH)_2$B-R]$^+$ and [^{99m}Tc$(CDOH)_3$B-R]$^{2+}$. However, it is more difficult to convert [^{99m}TcL(CDO)$(CDOH)_2$B-R] to [^{99m}Tc(CDO)$(CDOH)_2$B-R]$^+$ by ligand dissociation. This statement is supported by the fact that heating is needed to complete the ligand exchange reaction between [^{99m}TcCl(CDO)$(CDOH)_2$B-R] and sodium azide to form the ^{99m}Tc(III)-azide complexes [^{99m}Tc(N_3)(CDO)$(CDOH)_2$B-R]. Lipophilic cations, such as [^{99m}TcL$(CDOH)_3$B-R]$^+$ and [^{99m}Tc(CDO)$(CDOH)_2$B-R]$^+$, are able to localize and retain in mitochondria due to the negative potential ($\Delta\Psi = 120–180$ mV) across the inner mitochondrial membrane [40]. It would be difficult for [^{99m}Tc(CDO)$(CDOH)_2$B-R]$^{2+}$ to penetrate the rigid mitochondrial membranes due to its 2 positive charges (Chart II). This might explain the fact that complexes [^{99m}Tc(N_3)(CDO)$(CDOH)_2$B-R] tend to have longer heart retention.

One might wonder why the heart uptake values from planar image quantification are so different from those from biodistribution studies. The answer lies in the way of planar imaging. Firstly, the radioactivity from planar image quantification is accumulative over a specific period of time (e.g. 0–1 min) while the heart uptake from biodistribution is obtained at a specific time after administration of the radiotracer. Secondly, the heart uptake values from the planar image quantification include parts of the radioactivity in blood pool and surrounding normal tissues (background). While the heart uptake values can be corrected by deducting the radioactivity in normal organ above or beside the heart, it is impossible to separate the blood-bool radioactivity from that in the myocardium. Tissue γ-counting is the most accurate way to determine the heart uptake and biodistribution properties of a specific radiotracer at different time points. However, dynamic planar imaging

remains an important tool to compare the heart retention or myocardial washout kinetics of new ^{99m}Tc(III) radiotracers without sacrificing a large number of animals.

5. Conclusions

In conclusion, both boronate caps and azide coligand have significant impact on the radiochemistry, heart uptake and myocardial retention times of ^{99m}Tc(III)-azide complexes [^{99m}Tc(N_3)(CDO)$(CDOH)_2$B-R]. Among radiotracers evaluated in SD rats, ^{99m}Tc-ISboroxime-N_3 shows high initial heart uptake with the retention time comparable to that of ^{99m}Tc-Teboroxime. ^{99m}Tc-ISboroxime-N_3 is a promising alternative to ^{99m}Tc-Teboroxime for SPECT MPI. Our future research will focus on new ^{99m}Tc(III) radiotracers with a longer myocardial retention. High initial heart uptake and long myocardial retention will help to maintain the linear relationship between the radiotracer uptake and regional blood flow for an extended period, which is important for precise measurement of regional blood flow in cardiac patients.

Conflict of interest

Authors declare that they have no conflict of interest.

Acknowledgement

This work was supported, in part, by Purdue University, the grant R21 EB017237-01 (S.L.) from the National Institute of Biomedical Imaging and Bioengineering (NIBIB), the grant 81401446 from the National Nature Science Foundation of China (Y.Z.), and the grant 2219 (U.A.) from the Scientific and Technological Research Council of Turkey (TUBITAK).

References

[1] Di Carli MF, Hachamovitch R. New technology for noninvasive evaluation of coronary artery disease. Circulation 2007;115:1464–80.
[2] Baggish AJ, Boucher CA. Radiopharmaceutical agents for myocardial perfusion imaging. Circulation 2008;118:1668–74.
[3] Slomka PJ, Patton JA, Berman DS, Germano G. Advances in technical aspects of myocardial perfusion SPECT imaging. J Nucl Cardiol 2009;16:255–76.
[4] Salerno M, Beller GA. Noninvasive assessment of myocardial perfusion. Circ Cardiovasc Imaging 2009;2:412–24.
[5] Stirrup J, Wechalekar K, Maenhout A, Anagnostopoulos C. Cardiac radionuclide imaging in stable coronary artery disease and acute coronary syndromes. Br Med Bull 2009;89:63–78.
[6] Gaemperli O, Kaufmann PA. Lower dose and shorter acquisition: pushing the boundaries of myocardial perfusion SPECT. J Nucl Cardiol 2011;18:830–2.
[7] Perrone-Filardi P, Costanzo P, Dellegrottaglie S, Gargiulo P, Ruggiero D, Savarese G, et al. Prognostic role of myocardial single photon emission computed tomography in the elderly. J Nucl Cardiol 2010;17:310–5.
[8] Bailey DL, Willowson KP. An evidence-based review of quantitative SPECT imaging and potential clinical applications. J Nucl Med 2013;54:83–9.
[9] Nekolla SG, Rischpler C, Nakajima K. Myocardial blood flow quantification with SPECT and conventional tracers: a critical appraisal. J Nucl Cardiol 2014;21:1289–91.
[10] Hajjiri MM, Leavitt MB, Zheng H, Spooner AE, Fischman AJ, Gewirtz H. Comparison of positron emission tomography measurement of adenosine-stimulated absolute myocardial blood flow versus relative myocardial tracer content for physiological assessment of coronary artery stenosis severity and location. JACC Cardiovasc Imaging 2009;2:751–8.
[11] Jurisson SS, Hirth W, Linder KE, Di Rocco RJ, Narra RK, Nowotnik DP, et al. Chloro → hydroxy substitution on technetium BATO [TcCl(dioxime)$_3$ BR] complexes. Int J Rad Appl Instrum B 1991;18:735–44.
[12] Seldin DW, Johnson LL, Blood DK, Muschel MJ, Smith KF, Wall RM, et al. Myocardial perfusion imaging with technetium-99m SQ30217: comparison with thallium-201 and coronary anatomy. J Nucl Med 1989;30:312–9.
[13] Leppo JA, Meerdink DJ. Comparative myocardial extraction of two technetium-labeled BATO derivatives (SQ30217, SQ32014) and thallium. J Nucl Med 1990;31:67–74.
[14] Marshall RC, Leidholdt Jr EM, Zhang DY, Barnett CA. The effect of flow on technetium-99m-teboroxime (SQ30217) and thallium-201 extraction and retention in rabbit heart. J Nucl Med 1991;32:1979–88.
[15] McSherry BA. Technetium-99m-Teboroxime: a new agent for myocardial perfusion imaging. J Nucl Med Technol 1991;19:22–6.
[16] Iskandrian AS, Heo J, Nguyen T, Mercuro J. Myocardial imaging with Tc-99m teboroxime: technique and initial results. Am Heart J 1991;121:889–94.
[17] Rumsey WL, Rosenspire KC, Nunn AD. Myocardial extraction of teboroxime: effects of teboroxime interaction with blood. J Nucl Med 1992;33:94–101.
[18] Beanlands R, Muzik O, Nguyen N, Petry N, Schwaiger M. The relationship between myocardial retention of technetium-99m teboroxime and myocardial blood flow. J Am Coll Cardiol 1992;20:712–9.
[19] Williams KA, Taillon LA, Draho JM, Foisy MF. First-pass radionuclide angiographic studies of left ventricular function with technetium-99m-teboroxime, technetium-99m-sestamibi and technetium-99m-DTPA. J Nucl Med 1993;34:394–9.
[20] Johnson LL. Myocardial perfusion imaging with technetium-99m-teboroxime. J Nucl Med 1994;35:689–92.
[21] Kaufmann PA, Gaemperli O. Combining CT and nuclear: a winning hybrid team. J Nucl Cardiol 2009;16:170–2.
[22] Esteves FP, Raggi P, Folks RD, Keidar Z, Askew JW, Rispler S, et al. Novel solid-state-detector dedicated cardiac camera for fast myocardial perfusion imaging: multicenter comparison with standard dual detector cameras. J Nucl Cardiol 2009;16:927–34.
[23] Buechel RR, Pazhenkottil AP, Herzog BA, Husmann L, Nkoulou RN, Burger IA, et al. Real-time breath-hold triggering of myocardial perfusion imaging with a novel cadmium-zinc-telluride detector gamma camera. Eur J Nucl Med Mol Imaging 2010;37:1903–8.
[24] Duvall WL, Croft LB, Godiwala T, Ginsberg E, George T, Henzlova MJ. Reduced isotope dose with rapid SPECT MPI imaging: initial experience with a CZT SPECT camera. J Nucl Cardiol 2010;17:1009–14.
[25] Pazhenkottil AP, Buechel RR, Herzog BA, Nkoulou RN, Valenta I, Fehlmann U, et al. Ultrafast assessment of left ventricular dyssynchrony from nuclear myocardial perfusion imaging on a new high-speed gamma camera. Eur J Nucl Med Mol Imaging 2010;37:2086–92.
[26] Schillaci O, Danieli R. Dedicated cardiac cameras: a new option for nuclear myocardial perfusion imaging. Eur J Nucl Med Mol Imaging 2010;37:1706–9.
[27] Fiechter M, Ghadri JR, Kuest SM, Pazhenkottil AP, Wolfrum M, Nkoulou RN, et al. Nuclear myocardial perfusion imaging with a novel cadmium-zinc-telluride detector SPECT/CT device: first validation versus invasive coronary angiography. Eur J Nucl Med Mol Imaging 2011;38:2025–30.
[28] van Dijk JD, Jager PL, Mouden M, Slump CH, Ottervanger JP, de Boer J, et al. Development and validation of a patient-tailored dose regime in myocardial perfusion imaging using CZT-SPECT. J Nucl Cardiol 2014;21:1158–67.
[29] Mouden M, Ottervanger JP, Knollema S, Timmer JR, Reiffers S, Oostdijk AH, et al. Myocardial perfusion imaging with a cadmium zinc telluride-based gamma camera versus invasive fractional flow reserve. Eur J Nucl Med Mol Imaging 2014;41:956–62.
[30] Ward RP, Al-Mallah MH, Grossman GB, Hansen CL, Hendel RC, Kerwin TC, et al. American Society of Nuclear Cardiology review of the ACCF/ASNC appropriateness criteria for single-photon emission computed tomography myocardial perfusion imaging (SPECT MPI). J Nucl Cardiol 2007;14:e26–38.
[31] Garcia EV, Gropler RJ. Ninth nuclear cardiology invitational conference, Annapolis, Maryland, 2008. J Nucl Cardiol 2008;15:e37–50.
[32] Underwood SR, de Bondt P, Flotats A, Marcasa C, Pinto F, Schaefer W, et al. The current and future status of nuclear cardiology: a consensus report. Eur Heart J Cardiovasc Imaging 2014;15:949–55.
[33] Liu S, He Z, Hsieh WY, Kim YS. Evaluation of novel cationic ^{99m}Tc-nitrido complexes as radiopharmaceuticals for heart imaging: improving liver clearance with crown ether groups. Nucl Med Biol 2006;33:419–32.
[34] Kim YS, He Z, Hsieh WY, Liu S. A novel ternary ligand system useful for preparation of cationic ^{99m}Tc-diazenido complexes and ^{99m}Tc-labeling of small biomolecules. Bioconjug Chem 2006;17:473–84.
[35] He Z, Hsieh WY, Kim YS, Liu S. Evaluation of novel cationic ^{99m}Tc(I)-tricarbonyl complexes as potential radiotracers for myocardial perfusion imaging. Nucl Med Biol 2006;33:1045–53.
[36] Kim YS, He Z, Hsieh WY, Liu S. Impact of bidentate chelators on lipophilicity, stability, and biodistribution characteristics of cationic ^{99m}Tc-nitrido complexes. Bioconjug Chem 2007;18:929–36.
[37] Liu S. Ether and crown ether-containing cationic ^{99m}Tc complexes useful as radiopharmaceuticals for heart imaging. Dalton Trans 2007;28:1183–93.
[38] Kim YS, Wang J, Broisat A, Glover DK, Liu S. Tc-99m-N-MPO: novel cationic Tc-99m radiotracer for myocardial perfusion imaging. J Nucl Cardiol 2008;15:535–46.
[39] Fang W, Liu Y, Zhu L, Kim YS, Liu S, He ZX. Evaluation of ^{99m}TcN-15C5 as a new myocardial perfusion imaging agent in normal dogs and canines with coronary stenosis. Nucl Med Commun 2008;29:775–81.
[40] Kim YS, Shi J, Zhai S, Hou G, Liu S. Mechanism for myocardial localization and rapid liver clearance of Tc-99m-N-MPO: a new perfusion radiotracer for heart imaging. J Nucl Cardiol 2009;16:571–9.
[41] Liu Z, Chen L, Liu S, Barber C, Stevenson GD, Furenlid LR, et al. Kinetic characterization of a novel cationic ^{99m}Tc(I)-tricarbonyl complex, ^{99m}Tc-15C5-PNP, for myocardial perfusion imaging. J Nucl Cardiol 2010;17:858–67.
[42] Bu L, Li R, Jin Z, Wen X, Liu S, Yang B, et al. Evaluation of ^{99m}TcN-MPO as a new myocardial perfusion imaging agent in normal dogs and in an acute myocardial infarction canine model: comparison with ^{99m}Tc-Sestamibi. Mol Imaging Biol 2011;13:121–7.
[43] Zheng Y, Ji S, Tomaselli E, Liu S. Development of formulations for ^{99m}TcN-MPO: a cationic radiotracer for myocardial perfusion imaging. J Labelled Comp Radiopharm 2014;57:584–92.
[44] Zheng Y, Ji S, Tomaselli E, Ernest C, Freiji T, Liu S. Effect of co-ligands on chemical and biological properties of ^{99m}Tc(III) complexes [^{99m}Tc(L)(CDO)$(CDOH)_2$BMe] (L = Cl, F, SCN and N_3; $CDOH_2$ = cyclohexanedione dioxime). Nucl Med Biol 2014;41:813–24.

[45] Yang Y, Zheng Y, Tomaselli E, Fang W, Liu S. Impact of boronate capping groups on biological characteristics of novel ^{99m}Tc(III) complexes [^{99m}TcCl(CDO)(CDOH)$_2$B-R] (CDOH$_2$ = cyclohexanedione dioxime). Bioconjug Chem 2015;26:316–38.

[46] Jurisson S, Francesconi L, Linder KE, Treher E, Malley MF, Gougoutas JZ, et al. Syntheses, characterization, and reactivity of manganese and rhenium dioxime complexes. X-ray crystal structures of Mn^{II}(CDO) (CDOH)$_2$(BPh(OCH$_3$))$_2$, an unusual pseudoclathrochelate complex, and Re^{III}Cl(CDO)(CDOH)$_2$BPh. Inorg Chem 1991;30:1820–7.

[47] Treher EN, Francesconi LC, Gougoutas JZ, Malley MF, Nunn AD. Monocapped Tris(dioxime) complexes of technetium(III): synthesis and structural characterization of TcX(dioxime)$_3$B-R (X = Cl, Br; dioxime = dimethylglyoxime, cyclohexanedione dioxime; R = CH$_3$, C$_4$H$_9$). Inorg Chem 1989;28:3411–6.

[48] Jurisson S, Halihan MM, Lydon JD, Barnes CL, Nowotnik DP, Nunn AD. Linkage isomerization of MSCN(CDOH)$_2$(CDO)BMe to MNCS(CDOH)$_2$(CDO)BMe (M = Tc, Re). crystal structures of TcNCS(CDOH)$_2$(CDO)BMe, ReNCS(CDOH)$_2$(CDO)BMe, and ReSCN(CDOH)$_2$(CDO)BMe. Inorg Chem 1998;37:1922–8.

[49] Carvalho PA, Chiu ML, Kronauge JF, Kawamura M, Jones AG, Holman BL, et al. Subcellular distribution and analysis of technetium-99m-MIBI in isolated perfused rat hearts. J Nucl Med 1992;33:1516–22.

[50] Bolzati C, Cavazza-Ceccato M, Agostini S, Tokunaga S, Casara D, Bandoli G. Subcellular distribution and metabolism studies of the potential myocardial imaging agent [^{99m}Tc(N)(DBODC)(PNP5)]$^+$. J Nucl Med 2008;49:1336–44.

[51] Younes A, Songadele JA, Maublant J, Platts E, Pickett R, Veyre A. Mechanism of uptake of technetium-tetrofosmin II: uptake into isolated adult rat heart mitochondria. J Nucl Cardiol 1995;2:327–33.